

EFFECT OF THE AMBIPOLAR POTENTIAL ON STELLARATOR CONFINEMENT

H.E. MYNICK, W.N.G. HITCHON
Torsatron/Stellarator Laboratory,
University of Wisconsin,
Madison, Wisconsin,
United States of America

ABSTRACT. The confinement properties of reactor-scale stellarators in the presence of a self-consistent ambipolar potential Φ are examined in the light of the current theoretical expectations for the dependence of the transport coefficients on collisionality and radial electric field. It is found that stellarators have sufficiently good confinement to be viable as reactors. In addition, it is found that multiple roots of the ambipolarity constraint can exist in stellarators (as in other devices) and that, for appropriate parameters, confinement can be improved by operating at a root different from the one usually considered.

1. INTRODUCTION

In this paper we consider the effect on transport of the ambipolar potential $\Phi(r)$ in a stellarator with reactor-like parameters. The basic conceptual approach we use is similar to previous work [1, 2] in stellarator transport. Given expressions for the particle fluxes Γ_1^s for electrons ($s=e$) and ions ($s=i$) as a function of radial electric field, $E_r = -\Phi'(r)$, E_r is determined self-consistently by imposing the ambipolarity constraint $\Gamma_1^e = \Gamma_1^i$. This value of E_r is then used to determine both the particle and heat fluxes.

The present work has a number of features, however, in which more recent developments in transport theory are utilized. The appropriate expressions for transport coefficients at low collisionality (or strong electric field) [3, 4] are different from those employed in Refs [1, 2]. Also, the fact that particles of the same species but with different energies contribute to different transport regimes has been taken account of here, in contrast to Ref. [1].

In addition, it is shown here that for appropriate parameters, multiple roots Φ_j ($j = 1, 2, 3$) of the ambipolarity constraint exist. Multiple roots have previously been found for the Elmo Bumpy Torus [5] and more recently for tandem mirrors [6]. Of the roots which are stable to radial fluctuations in charge density, the one (Φ_1) which is present for all device parameters is that for which the ions are held in by the electrons ($\Phi(r=0)$ negative). It is this root to which the system should move, if started with $\Phi(t=0) = 0$, and with $T_i \cong T_e$, and it is the root normally looked at [1, 2].

For suitable parameters, however, there is a second stable root Φ_2 , at positive Φ and of substantially larger magnitude, and the confinement times for this root can be significantly longer than those for Φ_1 . Thus it is of interest to consider when this root may be accessed in an experimental situation and how much improvement may be obtained.

In view of these developments, and particularly in view of the renewed interest in whether stellarators possess sufficiently good confinement to make viable reactors, a reassessment of the theoretical expectations for stellarator confinement times seems warranted. We find that acceptably long confinement times ($\tau_E \geq 1$ s) can be achieved for reasonable reactor parameters, though by only a modest margin.

In Section 2 we describe the transport model and assumptions going into the results presented in the following sections. Section 3 presents results for a reactor-size stellarator and discusses the physics and parametric dependences of the standard root Φ_1 . In Section 4 the possibility of operation at the second stable root is investigated. Some summarizing comments are made in Section 5.

2. THE TRANSPORT MODEL

The results presented in Sections 3 and 4 are plots of the expected particle and energy fluxes versus $\phi_i' \equiv e\Phi'/T_i$, where $e \equiv e_i$ is the ion charge and T_i the ion temperature. The fluxes come from doing the

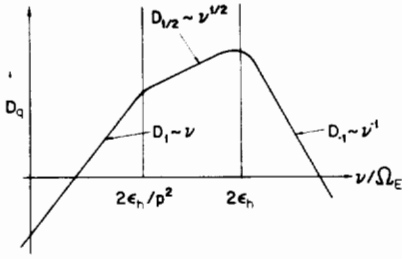


FIG. 1. Log-log plot of diffusion coefficient D_q versus ν/Ω_E , showing the three low-collisionality regimes ($q = -1, 1/2, 1$) used in the text.

appropriate energy integral over the three low-collisionality regimes [1-4] of transport, shown in Fig. 1 (axes are log-log). For particles with kinetic energy $E = Mv^2/2$, the transport coefficients are given by

$$D_{-1}(E) = \sigma_{-1} (2\epsilon_h)^{3/2} v_B^2 / \nu = D_{-1T} x^{7/2} \quad (1)$$

$$D_{1/2}(E) = \sigma_{1/2} \nu^{1/2} v_B^2 / \Omega_E^{3/2} = D_{1/2T} x^{5/4} \quad (2)$$

$$D_1(E) = \sigma_1 \nu p v_B^2 / [\Omega_E^2 (2\epsilon_h)^{1/2}] = D_{1/2T} x^{1/2} \quad (3)$$

where $p \equiv \epsilon_h/\epsilon_t$, $\epsilon_h(r)$ is the helical ripple amplitude, $\epsilon_t(r) = r/R_0$ is the inverse aspect ratio, $x \equiv E/T$, Ω_E is the $E \times B$ poloidal precession frequency, $v_B \propto x$ is the radial grad-B drift, $\nu \approx \nu_T x^{-3/2}$ is the collision frequency for a particle with energy E , ν_T is the thermal collision frequency, and $D_{qT} \equiv D_q(E = T)$, for each of $q = -1, 1/2, 1$. Here, q is the power of ν appearing in D_q in Eqs (1-3). The σ_q here are numerical coefficients arising from kinetic theory, given by $\sigma_{-1} \approx 0.65$, $\sigma_{1/2} \approx 1.67$ and $\sigma_1 \approx 1.0$.

For any function $g(E)$, the radial flux Γ_g of g is (species label suppressed)

$$\begin{aligned} \Gamma_g &= -4\pi \int dv v^2 [g(E) D(E) \partial_r f_0] \\ &= -2^{1/2} 4\pi v_T^3 \int dx x^{1/2} g D \partial_r f_0 \end{aligned} \quad (4)$$

where

$$\begin{aligned} \partial_r f_0 &= \frac{n_0}{(2\pi)^{3/2} v_T^3} e^{-x} \\ &\times [\partial_r \ln n_0 + \phi' + \partial_r \ln T (x - \frac{3}{2})] \end{aligned} \quad (5)$$

Here, $\phi' \equiv \phi'_s \equiv e_s \partial_r \Phi / T_s$ ($s = e, i$). From Eq.(4), Γ_1 is the particle flux and $\Gamma_E = T\Gamma_x$ is the energy flux. Putting Eq.(5) into Eq.(4), one has

$$\begin{aligned} \Gamma(x^r) &= - \left(\frac{2}{\sqrt{\pi}} n_0 \right) \\ &\times \sum_q D_{qT} \{ [\partial_r \ln n_0 + \phi'] I(x, n_q) |_{\pm}^+ \\ &+ \partial_r \ln T [I(x, n_{q+1}) - \frac{3}{2} I(x, n_q)] |_{\pm}^+ \} \end{aligned} \quad (6)$$

where

$$n_q \equiv \frac{5}{2} - \frac{3}{2} q + r \quad (7)$$

is the power of x occurring in the integral (4), yielding the integral

$$I(x, n) \equiv \int^x dx_1 x_1^n e^{-x_1} \quad (8)$$

to be evaluated. $I(x, n)$ satisfies the recursion relation

$$I(x, n) = -x_1^n e^{-x_1} |_{\pm}^x + n I(x, n-1) \quad (9)$$

Thus, for n an integer,

$$I(x, n) = -n! \left(\frac{x^n}{n!} + \frac{x^{n-1}}{(n-1)!} + \dots + \frac{1}{0!} \right) e^{-x} \quad (10a)$$

and for any $n > 0$,

$$I(x, n) |_0^\infty = \Gamma(n+1) \equiv n! \quad (10b)$$

with $\Gamma(n)$ the usual gamma function. The limits ' \pm ' in Eq.(6) denote the upper and lower boundaries of the three q -regions, determined by the values of x for which the D_q 's for two neighbouring q -values are equal. For $p \equiv \epsilon_h/\epsilon_t > 1$, all three D_q 's contribute. For $p < 1$, only D_{-1} and D_1 contribute, since the width of the $q = \frac{1}{2}$ region vanishes.

It will be useful to denote the term in $\{ \}$ in Eq.(6) by a symbol ' F_{gq} ',

$$\{ \} \equiv n_q! F_{gq}/q \quad (11)$$

' F ' stands for the thermodynamic 'force' from the q -contribution to flux Γ_g . It is normalized to be dimensionless and is independent of T_s , n_0 or minor radius a .

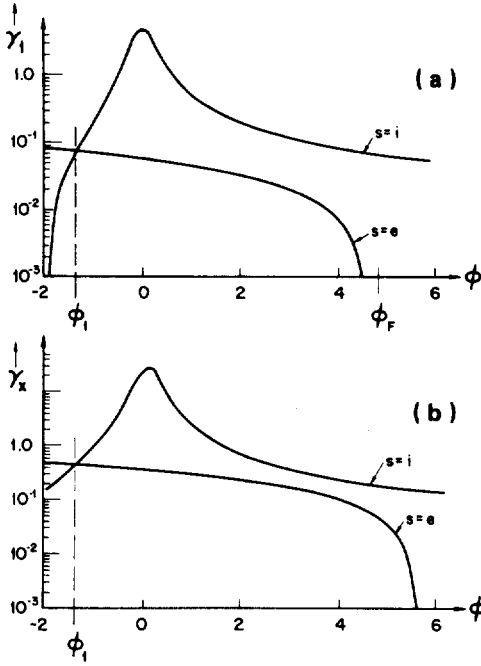


FIG. 2. Plots of the normalized particle fluxes γ_1^s (a) and energy fluxes γ_x^s (b) versus potential ϕ for a stellarator with $n = 10^{14} \text{ cm}^{-3}$, $T_e = T_i = 10 \text{ keV}$, $B = 5 \text{ T}$, $a = 2.5 \text{ m}$, $\epsilon_a = 0.1$ and $\epsilon_h = 0.05$ at $r/a = 0.5$. Shown is the single root ϕ_1 to the ambipolarity constraint, and the point ϕ_F at which the electron flux becomes negative.

3. OPERATION AT Φ_1

In the following results, Γ_g is normalized to $\gamma_g \equiv \Gamma_g / (n_0 a)$, which has units of s^{-1} . The confinement times are then given by

$$\tau_g \approx \gamma_g^{-1} \tag{12}$$

The usual tokamak formula is $\tau_E \approx a^2 / 4\chi_E \approx 1/4\gamma_x$. The factor-of-four enhancement in γ_g in Eq.(12) is to approximately account for the much stronger T-dependence of D_q compared with the tokamak transport coefficients. This tends to flatten the T(r)-profile to a form like $[J_0(2.404 r/a)]^{1/m_q}$, where $1 < m_q \sim n_q$, instead of the tokamak formula, for which $m_q = 1$.

We begin by plotting $\gamma_{1,x}$ versus $\phi \equiv a\phi_1'$ for a reactor-like configuration in Fig. 2, for which $n = 10^{14} \text{ cm}^{-3}$, $T_i = T_e = 10 \text{ keV}$, $B = 5 \text{ T}$, $a = 2.5 \text{ m}$, $\epsilon_a \equiv \epsilon_t(\rho = 1) = 0.1$ and $\epsilon_h(\rho) = 0.05$ at $\rho \equiv r/a = 0.5$, so that $p(\rho = 0.5) = \epsilon_h(0.5) / \epsilon_t(0.5) = 1$. Ambipolarity is satisfied at the single root $\phi = \phi_1 \approx -1.4$, at which $\tau_{11} = \gamma_{11}^{-1} \approx 13 \text{ s}$, $\tau_{x1}^e = (\gamma_{x1}^e)^{-1} \approx 2.2 \text{ s}$ and $\tau_{x1}^i \approx 2.2 \text{ s}$.

(Here the first subscript (1,x) refers to g, and the second subscript (1 only here) refers to the root number.) This single root is the one considered in Refs [1] and [2] (though there it was assumed that $D_{1/2}$, rather than the present D_1 , is the form which applies at large x).

At root 1, the electrons are mostly in the $q = -1$ (ν^{-1}) regime and hold in the ions, which are principally in the $q = 1$ regime. The modest size of $|\phi_1|$ is due to the fall-off of D_1 with increasing $|\phi|$ or Ω_E , and also to the weak energy dependence of D_1 , which causes the ion forces $F_{1,x}^i$ to become negative at fairly small $|\phi|$.

The principal point of Fig. 2 is that $\tau_x \geq 1 \text{ s}$ is achievable with reasonable reactor parameters, though not by a large margin. Additional enhancement of τ_x could come from a number of factors:

- (a) Further adjustment of parameters, using the fact that $\gamma_{x1}^e \sim \epsilon_h^{3/2} \epsilon_a^2 T_e^{7/2} B^{-2} n_0^{-1} a^{-4}$. For example, sufficient rotational transform could be obtained for a stellarator with half the ϵ_h used in Fig. 2 [7]. The density could realistically be doubled. Operating at only 8 keV would enhance τ_{x1}^e by an additional factor of two.
- (b) Tailoring of the magnetic fields to minimize the (velocity-space-averaged) radial drift velocity of helically trapped particles [8]. Another order of magnitude in τ_x could possibly be derived from such optimization.
- (c) An 'enhancement factor' greater than the factor of four used in Eq.(12) may be appropriate, to account for the weaker fall-off (except near the edge) of T(r). One-dimensional solutions of the transport equations would answer more definitively whether the factor of four is adequate or not.
- (d) Operating at a different root of the ambipolarity equation. This possibility is discussed next.

4. MULTIPLE ROOTS

Figure 3 shows γ_1 and γ_x for $a = 1 \text{ m}$ (otherwise the same parameters are used as for Fig. 2). Here a new possibility is illustrated. One sees that the ambipolarity condition $\gamma_1^i = \gamma_1^e$ is met at *three* values of ϕ , of which two, labelled ϕ_1 and ϕ_2 , are stable, as already mentioned. In contrast to $\phi_1 \approx -0.4$, at root 2, $\phi_2 \approx 3.3$ is positive and rather large. Here, the ions hold in the electrons, which require a large potential because of the strong energy dependence of $D_{-1}^e \propto x^{7/2}$. This large potential in turn greatly diminishes $D_1^i \propto \phi^{-2}$,

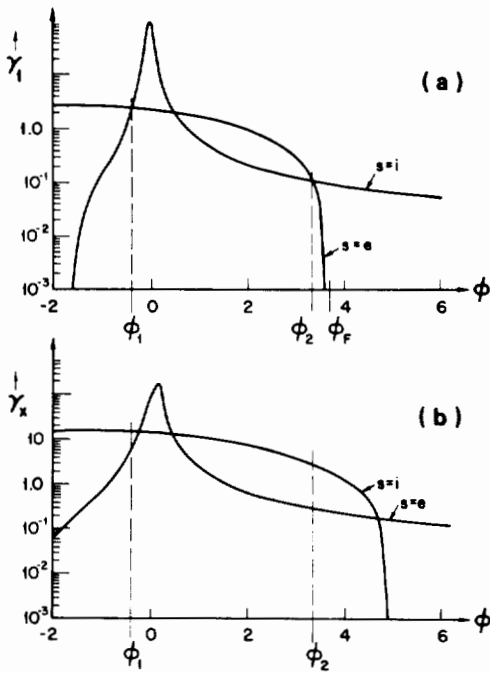


FIG. 3. Same as Fig. 2, but for $a = 1$ m. The second stable root ϕ_2 present for these parameters is indicated.

which permits the electrons to escape more rapidly than the ions in the first place.

The most significant feature of root 2 here is that its confinement is much better than that of root 1. One sees that $\tau_{11} \cong 0.65$ s, $\tau_{x1}^e \cong 0.07$ s and $\tau_{x1}^i \cong 0.18$ s, while $\tau_{12} \cong 7.7$ s, $\tau_{x2}^e \cong 0.31$ s and $\tau_{x2}^i \cong 2.9$ s, so that $\tau_{12}/\tau_{11} \cong 12$, $\tau_{x2}^e/\tau_{x1}^e \cong 4.4$ and $\tau_{x2}^i/\tau_{x1}^i \cong 16$.

Since a is only one metre in Fig. 3, one might hope to achieve $\tau_x \geq 1$ s simply by increasing a to a more typical reactor-size value. In Figs 2 and 4 are shown the $\gamma_{1,x}$ curves for the scaled-up versions of Fig. 3, with $a = 2.5$ and 1.6 m, respectively. One notes a loss of roots 2 and 3, with $a = 1.6$ m being approximately the marginal point at which these two roots coalesce and then vanish. As that point is approached, the relative advantage of root 2 over root 1 is diminished. In Fig. 4, $\tau_{12}/\tau_{11} \cong 5.1/2.4 = 2.1$, $\tau_{x2}^e/\tau_{x1}^e \cong 0.71/0.4 = 1.8$ and $\tau_{x2}^i/\tau_{x1}^i \cong 2.0/0.65 = 3.1$.

Pictorially, the reason for the loss of roots is that the ion fluxes fall off more slowly with ϕ as a increases, so that Γ_1^i cannot become smaller than $\Gamma_1^e \propto D^e F_1^e$ before $F_1^e(\phi)$ becomes negative, at $\phi = \phi_F$ (indicated in Figs 2–4). Physically, this broadening of the ion peak in $\Gamma^i(\phi)$ occurs for the following reason: If a is doubled (but Φ or ϕ kept constant), Ω_E is reduced by 1/4 (half as large an $E \times B$ velocity v_E and twice as far to drift). Since the potential strength needed to reduce D^i from D_{-1}^i to $D_{1/2,1}^i$ is given by $1 \cong \nu_{hi}/\Omega_E$ ($\nu_{hs} \equiv \nu_s/2\epsilon_h$), doubling a broadens the $\Gamma^i(\phi)$ peak by roughly 4. In

other words, the size of Φ is governed by the operating temperature T , and not by the linear dimension ($\propto a$) of the device. Thus, if a is varied, one sees that T should also be scaled in some fashion, if the transport characteristics are to remain the same.

To make these ideas more precise, we develop an explicit form for the ambipolarity equation. We assume that the ions are entirely in the $q = 1$ regime and the electrons in the $q = -1$ regime. In the vicinity of $\phi = 0$, where the ions should actually have $q = -1$, $\Gamma^i \gg \Gamma^e$, so no roots occur in this region anyway. Roots 2 and 3 will thus occur if

$$1 \leq \frac{\Gamma_1^e}{\Gamma_1^i} = \frac{n_{-1}^i}{n_1^i} \frac{D_{-1}^e T}{D_{1T}^i(\phi)} \frac{F_1^e(\phi)}{F_1^i(\phi)} \quad (13)$$

for some interval of $\phi > 0$. The places where ϕ enters are explicitly noted in Eq.(13). With the inequality in Eq.(13) replaced by an equality, Eq.(13) is the equation for the roots $\phi_{1,2,3}$. As will be seen shortly, Eq.(13) is cubic in ϕ . From Eq.(11),

$$F_1^e(\phi) = a[K_n + (n_{-1} - \frac{1}{2})K_T] - \left(\frac{T}{T_i}\right)\phi$$

$$\cong \frac{T}{T_i} (\phi_F - \phi) \quad (14a)$$

$$F_1^i(\phi) = a[K_n + (n_1 - \frac{1}{2})K_T] + \phi \equiv \phi_{F1} + \phi \quad (14b)$$

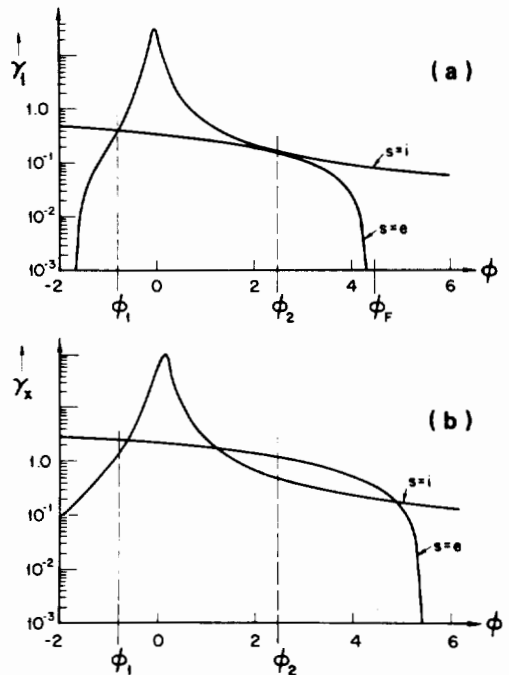


FIG. 4. Same as Fig. 3, but for $a = 1.6$ m.

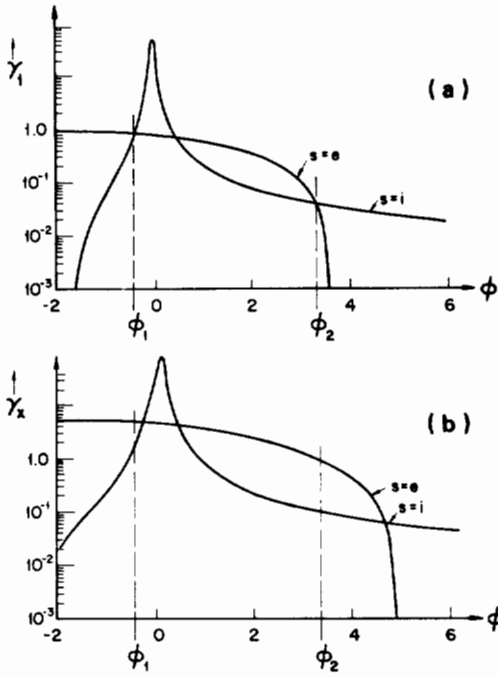


FIG. 5. Same as Fig. 3, but for $a = 2.5$ m, $T = 20.8$ keV.

where $K_{n,T} \equiv \partial_r \ln(n_0, T)$, ϕ_F is the value of ϕ at which $F_1^e = 0$ (as already noted), and similarly for the ion counterpart $-\phi_{Fi}$.

One has

$$\Omega_E = \Omega_E' \phi \tag{15a}$$

where

$$\Omega_E' \equiv \partial_\phi \Omega_E = \frac{a}{r} \left(\frac{\rho_s}{a}\right)^2 \Omega_s = 10^4 \left[\frac{a}{r} \frac{T_s}{Ba^2} \right] s^{-1} \tag{15b}$$

In the final form here, the units are: T_s (10 keV), B (T), a (m). Similarly, we write

$$v_s \approx 1.2 \times 10^2 \left[\left(\frac{m_i}{m_s}\right)^{1/2} n_s T_s^{-3/2} \right] \tag{16}$$

Thus, from Eqs (1) and (3),

$$\frac{n_{-1}^e}{n_1^e} \frac{D_{-1T}^e}{D_{1T}^e} = \frac{4!}{1!} \left(\frac{m_e}{m_i}\right)^{1/2} \frac{1}{p} \left(\frac{2\varepsilon_H \Omega_E'}{v_i}\right)^2 \phi^2 \equiv d\phi^2 \tag{17}$$

where

$$d = 0.39 \times 10^4 \left[\frac{1}{p} \left(\frac{(2\varepsilon_H) T_i^{5/2}}{\left(\frac{r}{a}\right) B a^2 n_0} \right)^2 \right] \tag{18}$$

with the parameters in square brackets here in the same units as in Eqs (15b) and (16). (Thus, for example, for the parameters of Fig. 3, $d = 0.624 \sim 1.0$). Using Eqs (14a), (14b) and (17) in Eq. (13), therefore,

$$1 \leq \left(d \frac{T_e}{T_i}\right) \phi^2 \frac{(\phi_F - \phi)}{(\phi_{Fi} + \phi)} \tag{19}$$

With the equality holding in Eq. (19), this is a cubic in ϕ , as already noted. The inequality will hold (and so real roots $\phi_{2,3}$ will exist) for $d_1 \equiv (dT_e/T_i)$ large enough, i.e. for $\Gamma^i(\phi) \sim (d\phi^2)^{-1}$ sharply enough peaked.

The right-hand side of Eq. (19) is a maximum at

$$\phi_m = \left(\frac{\phi_F - 3\phi_{Fi}}{4} \right) + \left[\left(\frac{\phi_F - 3\phi_{Fi}}{4} \right)^2 + \phi_F \phi_{Fi} \right]^{1/2} \tag{20}$$

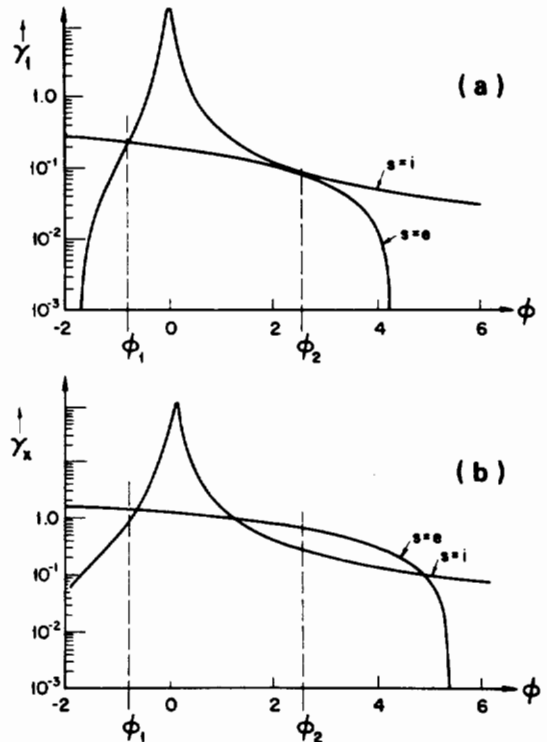


FIG. 6. Same as Fig. 3, but for $a = 2.5$ m, $T = 14.3$ keV.

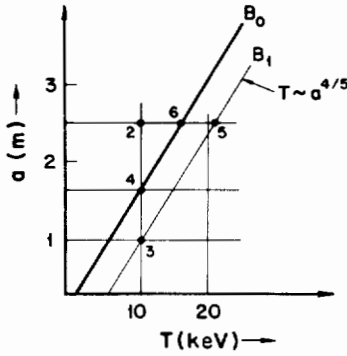


FIG. 7. Position in the (a, T) plane of the configurations of Figs 2–6. Configurations on the same line B_j are ‘homomorphic’ to one another.

Substituting this for ϕ in Eq.(19) yields an explicit criterion for the existence of roots 2,3.

Parameter variations leaving Eq.(19) unchanged provide useful scaling laws. Since from Eq.(18) $d \sim T_1^5/a^4$, while from Eq.(14) ϕ_F and ϕ_{Fi} are independent of T_s and a , one sees that if T and a are varied together so that $T \sim a^{4/5}$, Eq.(19) is unchanged, and the roots ϕ_j will also be unchanged. This is shown in Figs 5 and 6, in which Figs 3 and 4, respectively, are scaled in this fashion up to linear dimension $a = 2.5$ m. Thus $T = (2.5)^{4/5} (10 \text{ keV}) \cong 20.8 \text{ keV}$ for Fig.5 and $T = (2.5/1.6)^{4/5} (10 \text{ keV}) \cong 14.3 \text{ keV}$ for Fig.6. One notes that the shapes of the curves $\gamma_{1,x}^s(\phi)$ in Figs 5 and 6 are almost the same as those of Figs 3 and 4, but with the vertical scale changed (‘homomorphic’ configurations), indicating that our approximating both species as being entirely in a single q -regime is appropriate.

Figure 7 shows the position in the (a, T) plane of the set of configurations in Figs 2–6. Along the contours B_j are homomorphic configurations, satisfying $T \sim a^{4/5}$. B_0 is the configuration along which roots 2 and 3 marginally exist. Configurations to the left and above it must operate at root 1.

Typical values needed for a reactor are $a \sim 2$ m, $T \sim 10$ keV and $\tau_x \sim 1$ s. As illustrated by the points for Figs 2 and 6, for these required values the position in question is near or above the contour in B_0 in Fig.7. Thus, given these operating parameters, operation at root 2 instead of root 1 would seem to provide a relatively small enhancement of τ_x , of perhaps a factor of 2–3. The relative advantage might be much greater if some other set of reactor constraints (e.g. a larger plant output, or different fuel, requiring higher

operating temperature) demanded a plasma with larger d_1 .

In order to access root 2 experimentally, it would be necessary to develop an initial positive potential $\Phi(t = 0)$ greater than the unstable root Φ_3 . Once $\Phi > \Phi_3$ is achieved, the system will develop the remainder of the required potential by itself. One possible route to developing this initial positive ‘seed’ potential may be through heating the electrons first through ECRH, so that $D_{-1T}^e \gg D_{-1T}^i$. Then, for sufficiently low density that the ion-electron temperature equilibration is not too rapid, the required positive potential can be attained, and the plasma can then be brought up to operating density and temperature on the positive root.

5. DISCUSSION

From the results presented here, it appears that stellarators have sufficiently good confinement to make an acceptable reactor. A number of ways of enhancing the transport (while remaining within acceptable limits for operating parameters) have been noted, including the possibility of operation at an ambipolar potential which is large and positive.

The results presented here should be regarded as an initial reassessment of theoretical expectations for stellarators, given a number of new developments in stellarator theory. A number of additional refinements might also be helpful. The results here assume purely diffusive transport, neglecting the possibility of direct losses. Moreover, the present work is ‘zero-dimensional’; ϕ' and the fluxes are determined at a single radius r . As noted in Section 3, a one-dimensional solution, yielding radial profiles of all relevant parameters, would be useful to check the present zero-dimensional results. In this connection, we note that, if operation at ϕ_2 toward smaller r is desired, as the edge is approached and the temperature drops, it is likely that a loss of roots 2 and 3 will occur, requiring the plasma to make a transition to root 1. A similar phenomenon may occur in tandem mirrors [6], though this appears to be highly sensitive to geometry [9].

ACKNOWLEDGEMENTS

The authors are grateful to A.H. Boozer, P.J. Catto, J.H. Harris and M.N. Rosenbluth for useful discussions. This work was supported by the United States Department of Energy under Contract No.DE-AC02-78 ET53082.

REFERENCES

- [1] GALEEV, A.A., SAGDEEV, R.Z., FURTH, H.P., ROSENBLUTH, M.N., *Phys. Rev. Lett.* **22** (1969) 511.
- [2] KULSRUD, R.M., HO, D., in *Proc. Sherwood Theory Meeting, Santa Fe, NM* (1982), paper 1D9.
- [3] GALEEV, A.A., SAGDEEV, R.Z., *Rev. Plasma Phys.* **7** (1979) 257.
- [4] MYNICK, H.E., *Effect of Collisionless Detrapping on Superbanana Transport in a Stellarator with Radial Electric Field*, Univ. of Wisconsin Rep. TSL-83-1 (1983).
- [5] JAEGER, E.F., SPONG, D.A., HEDRICK, C.L., *Phys. Rev. Lett.* **44** (1978) 866.
- [6] MIRIN, A.A., AUERBACH, S.P., COHEN, R.H., GILMORE, J.M., PEARLSTEIN, L.D., RENSINK, M.E., *Nucl. Fusion* **23** (1983) 703.
- [7] HITCHON, W.N.G., JOHNSON, P.C., WATSON, C.J.H., *Parameter and Cost Optimisations for a Modular Stellarator Reactor*, UKAEA Culham Lab., Abingdon, Rep. CLM-P682 (1982).
- [8] MYNICK, H.E., CHU, T.K., BOOZER, A.H., *Phys. Rev. Lett.* **48** (1982) 322.
- [9] MYRA, J.R., CATTO, P.J., *Phys. Rev. Lett.* **48** (1982) 620.

(Manuscript received 22 February 1983)

Final manuscript received 5 May 1983)